Carbohydrate Polymers 115 (2015) 129–138

Contents lists available at ScienceDirect

Carbohydrate Polymers

journal homepage: www.elsevier.com/locate/carbpol

Study of the physical properties of calcium alginate hydrogel beads containing vineyard pruning waste for dye removal

X. Vecino [a], R. Devesa-Rey [a,b], J.M. Cruz [a], A.B. Moldes [a,*]

[a] Chemical Engineering Department, School of Industrial Engineering (EEI), University of Vigo, Campus As Lagoas-Marcosende, 36310 Vigo-Pontevedra, Spain

[b] Defense University Center, Naval Academy, University of Vigo, Plaza de España 2, 36920 Marín-Pontevedra, Spain

ARTICLE INFO

Article history:
Received 22 May 2014
Received in revised form 5 August 2014
Accepted 10 August 2014
Available online 3 September 2014

Keywords:
Calcium alginate hydrogel beads
Vineyard pruning waste
Adsorption kinetics
Dyes
Roughness
Compactness

ABSTRACT

In this work the morphological and surface properties of a biocomposite formulated with vineyard pruning waste entrapped in calcium alginate hydrogel beads were studied. The formulation of the calcium alginate hydrogel beads, containing vineyard pruning waste, was based on the capacity of this green adsorbent to remove dye compounds from wastewater, observing that in the optimum condition (1.25% of cellulosic residue, 2.2% of sodium alginate and 0.475 mol L^{-1} $CaCl_2$) the percentage of dyes was reduced up to 74.6%. At lower concentration of $CaCl_2$, high-resolution optical images show that the elongation of the vineyard-alginate biocomposite decreased, whereas the compactness increased. Moreover, higher concentrations of cellulosic residue increased the biocomposite roundness in comparison with biocomposite without the cellulosic residue. Interferometric perfilometry analysis (R_a, R_q, R_z and R_t) revealed that high concentrations of $CaCl_2$ increased the roughness of the of the calcium alginate hydrogel beads observing vesicles in the external surface.

1. Introduction

Nowadays exists an important interest in the formulation of new composites within a perspective of a sustainable development (Avérous & Le Digabel, 2006; Janaki et al., 2012; Tran, Duri, Delneri, & Franko, 2013). Biocomposites are composite materials comprising at least one major component derived from a biological origin. Biological material such as natural fibers, based many of them on lignocellulosic residues, can be considered as environmentally friendly raw materials for the development of biocomposites. These biocomposites usually have an internal structure composed by a biodegradable polymer that allows the diffusion of solutes through the polymeric networks and at the same time it can adsorb different substances from a liquid stream. The potential applicability of cellulose-based biocomposites and nanocomposites is extended in a wide range of applications such as packaging, pharmacology, cosmetics and biomedical fields (Kalia et al., 2011; Thakur, Gupta, & Thakur, 2014a). Thus, some authors have proposed the synthesis of graft copolymers from natural cellulose fibers (Thakur, Thakur, & Gupta, 2013a, 2013b, 2013c, 2013d, 2014b). However, studies reporting formulations of calcium alginate hydrogel beads containing cellulose-based adsorbents for wastewater treatment or for the purification of valuable products in liquid-solid extractions are scarce.

Some authors have formulated composites consisting of activated carbon entrapped in calcium alginate beads (Devesa-Rey, Bustos, Cruz, & Moldes, 2011; Vecino, Devesa-Rey, Moldes, & Cruz, 2012), whereas others authors have proposed the immobilization of renewable substrates like composted grape marc (Perez-Ameneiro, Vecino, Barbosa-Pereira, Cruz, & Moldes, 2014), peat (Vecino, Devesa-Rey, Cruz, & Moldes, 2013), or sawdust and sugarcane molasses (Gonte, Shelar, & Balasubramanian, 2013) for the removal of pigments from agro-industrial effluents. Despite, lignocellulose-based fibers can be used, in the formulation of biodegradable filler; the most of the published studies are based on biodegradable polyesters matrices (Avérous & Le Digabel, 2006).

On the other hand, some lignocellulosic residues like vineyard pruning waste can be fractionated in order to obtain hemicellulosic sugars that can be fermented to valuable products like lactic acid, biosurfactants or xylitol; remaining the solid fraction containing cellulose and lignin as a by-product of the fractionation process (Moldes, Torrado, Converti, & Domínguez, 2006; Moldes, Torrado, Barral, & Domínguez, 2007; Rivas, Torrado, Rivas, Moldes, & Domínguez, 2007; Rivera, Moldes, Torrado, & Domínguez, 2007).

* Corresponding author. Tel.: 34 986812022; fax: 34 986812201.
E-mail addresses: xanel.vecino@uvigo.es (X. Vecino), rosa.devesa.rey@cud.uvigo.es (R. Devesa-Rey), jmcruz@uvigo.es (J.M. Cruz), amoldes@uvigo.es (A.B. Moldes).

http://dx.doi.org/10.1016/j.carbpol.2014.08.088
0144-8617/

Thus, Bustos, Moldes, Cruz, and Domínguez (2004) hydrolysed vineyard pruning waste using acid hydrolysis with sulphuric acid to obtain hemicellulosic sugars (liquid phase), which can be used as a carbon source in fermentative process. However, during the acid hydrolysis a solid residue consisting of hydrolysed vineyard pruning waste was obtained as a residue.

The aim of this work is focused on the formulation and morphological study of an adsorbent consisting of hydrolysed vineyard pruning waste, entrapped in calcium alginate hydrogel beads, to remove dye compounds from winery wastewater. Several morphology and surfaces analysis like area, perimeter, as well as the elongation, roundness and compactness of vineyard-alginate biocomposite were studied before and after three cycles of adsorption–desorption. In addition, the roughness of calcium alginate hydrogel beads formulated with different doses of calcium chloride ($CaCl_2$) was studied.

2. Materials and methods

2.1. Extraction of the lignocellulosic fraction of vineyard pruning waste

Vineyard pruning waste was collected from local wine-producers (Galicia, North-West Spain). The lignocellulosic residue (cellulose, hemicellulose and lignin) was dried and milled (<1 mm), homogenized in a single batch and hydrolysed with 3% H_2SO_4 during 15 min at 130 °C with a liquid/solid ratio of 8:1 g/g (Bustos et al., 2004). After this treatment a solid phase composed by cellulose and lignin was obtained.

2.2. Characterization of the lignocellulosic fraction of vineyard pruning waste

The composition of the vineyard pruning waste was determined by quantitative hydrolysis following the procedure described in previous works (Cruz, Moldes, Bustos, Torrado, & Domínguez, 2007). The percentages of cellulose and hemicellulose in the solid fraction were calculated on the basis of monomeric sugars concentrations in the hydrolysates, glucose and xylose respectively, whereas the solid residue, obtained after hydrolysis, was considered as Klason lignin. Glucose and xylose in the liquid phase were analysed by high performance liquid chromatography (HPLC) with diode array detection (DAD) and refractive index detection (RID) (Agilent Technologies 1200 Series, Germany) using Rezex RHM-Monosaccharide H+ (8%) column (Phenomenex, USA) maintained at a constant temperature of 65 °C. The monomeric sugars were analysed using an isocratic elution, with Milli-Q water plus 0.005 N of H_2SO_4, at a flow rate of 0.4 mL min^{-1}.

2.3. Determination of dyes in wastewater

Agro-industrial effluents were collected from local wineries (Galicia, Spain). The color compounds of winery wastewater were evaluated using the color index (CI), measured as the sum of absorbance at 620, 520 and 420 nm and the CIE 1976 (L^*, a^*, b^*) or CIELAB color system, where L^* axis is associated with the lightness of the color and moves from 100 (white) to 0 (black). CIELAB color system is widely accepted by both the scientific community and industry, since it is the most 'perceptually uniform' of the color spaces (Berns, 2000; Völz, 2001). The CIELAB chromaticity diagram provides a color map on which the chromaticities of all colors are plotted (Vecino et al., 2012). Colorimetric analyses were carried out using a double-beam spectrophotometer (Jasco V-650, Spain).

2.4. Formulation of the vineyard-alginate biocomposite

A Box–Behnken factorial design Box and Behnken (1960) was applied for the formulation of a vineyard-alginate biocomposite, consisting of vineyard pruning waste entrapped in calcium alginate hydrogel beads, used in the treatment of wastewater contaminated with dye compounds. Table 1 includes the range of the independent variables studied. The standardized (coded) dimensionless independent variables used, with limits of variation (−1, 1), were defined as x_1 (coded concentration of cellulosic residue), x_2 (coded sodium alginate concentration) and x_3 (coded calcium chloride concentration); whereas the dependent variables consisted of color index (CI) reduction and lightness (L^*) named y_1 and y_2 respectively.

Table 1
Independent and dependent variables used in this study, including units, nomenclature and range.

Independent variables	Units	Nomenclature	Range and levels		
			−1	0	1
Cellulosic residue	%	x_1	0.5	1.25	2
Sodium alginate	%	x_2	1	3	5
Calcium chloride ($CaCl_2$)	mol L^{-1}	x_3	0.05	0.475	0.9

Different formulations of calcium alginate hydrogel beads, containing vineyard pruning waste, were prepared by mixing hydrolysed residue from vineyard pruning waste (0.5–2%) with different concentrations of sodium alginate (1–5%). These mixtures were then added drop-wise from a 1.5 mL pipette using a peristaltic pump (Masterflex 16L/S compact variable-speed pump, dual-channel, 115/230 VAC, Cole-Parmer, Spain) to different solutions of $CaCl_2$ (0.05–0.9 mol L^{-1}), which were used as a cross-linking solution.

2.5. Adsorption–desorption studies of vineyard pruning waste entrapped in calcium alginate hydrogel beads

Adsorption experiments were carried out in 250 mL Erlenmeyer flasks placed in an orbital shaker at 150 rpm and 25 °C. The solid/liquid ratio used was 1:1 (v/v). Samples were removed after 2 h, once the equilibrium was reached, for analysis of dye compounds.

Once the adsorption process finished, the agro-industrial effluent was filtered through a 0.45 μm pore size membrane (PTFE Hydrophilic, Advantec, Japan). The vineyard-alginate biocomposite was regenerated by washing it with distilled water at 100 °C during 30 min.

2.6. Morphology characterization of vineyard-alginate biocomposite

2.6.1. Scanning electron microscope (SEM) images of vineyard pruning waste entrapped in calcium alginate hydrogel beads

In order to obtain SEM images, the vineyard-alginate biocomposite was modified according to the procedure described below.

(i) Fixation: the biocomposite was washed with sodium cacodylate 0.1 mol L^{-1} buffer and fixed with 2.5% of glutaraldehyde in cacodylate 0.1 mol L^{-1} buffer during 2–4 h at 4 °C. Following, the vineyard-alginate biocomposite was introduced in 1% OsO_4 in cacodylate 0.1 mol L^{-1} buffer during 1 h at 4 °C.
(ii) Dehydration: it was carried out with ethanol using different graded series (30% – 1 × 15 min; 50% – 2 × 15 min; 70% – 2 × 15 min; 80% – 2 × 15 min; 90% – 2 × 15 min and 100% – 3 × 15 min).

(iii) Substitution: the biocomposite was introduced in amylacetate:ethanol in ordered series (1:3 – 2 × 15 min; 2:2 – 2 × 15 min; 3:1 – 2 × 15 min and amylacetate 100% – 3 × 15 min) in order to replace the ethanol for a liquid miscible with liquid CO_2.
(iv) Drying out: this step allows keeping intact the biocomposite structure replacing the internal liquid by gas using chamber critical point.

Finally, the samples were cut in liquid N_2, covered with gold and observed using SEM (Jeol JSM-6700F FEG) operating at an acceleration voltage of 5.0 kV for secondary-electron imaging (SEI).

2.6.2. Morphological analysis of the vineyard-alginate biocomposite using high-resolution optical images

High-resolution optical images of calcium alginate hydrogel beads, containing vineyard pruning waste, were obtained with a stereoscopic Microscopic SMZ 1500 (Nikon) using a objective lense HR Plan Apo 1× with eyepiece C-W 10×(F.N. 22), zoom range position 1× and 12 V/100 W halogen illuminator. This allows seeing and photographing any material, from macro views to high-magnification micro visualization, obtaining different measurements related with the size of the biocomposite (area, perimeter, major and minor axis, elongation, roundness and compactness) controlled by Image tool 3.00 software.

Thus, elongation was calculated as the ratio of the length of the major axis to the length of the minor axis. The major and minor axes are derived from an oriented bounding box containing the polygon. The elongation values of biocomposite were calculated following Eq. (1), whereas roundness was calculated using Eq. (2).

$$\text{Elongation} = \frac{\text{Major axis length}}{\text{Minor axis length}} \tag{1}$$

$$\text{Roundness} = \frac{4 \times \text{Area}}{\pi \times (\text{Major axis length})^2} \tag{2}$$

On the other hand, the compactness measure the circleness of an object based on the feret diameter. This is a group of diameters derived from the distance of two tangents to the contour of the particle in a well-defined orientation. If a particle has an irregular shape, the feret diameter usually varies much more than with regularly shaped particles. Basically the ratio of the feret diameter to the biocomposite's length it can range between 0 and 1. The compactness and feret diameter were calculated following Eqs. (3) and (4) respectively.

$$\text{Compactness} = \frac{\text{Feret diameter}}{\text{Major axis length}} \tag{3}$$

$$\text{Feret diameter} = \sqrt{\frac{4 \times \text{Area}}{\pi}} \tag{4}$$

2.6.3. Interferometric perfilometry analysis of calcium alginate hydrogel beads

Roughness parameters of calcium alginate hydrogel beads were obtained by interferometry perfilometry using a Wyko-Veeco (NT1100) that is a non-contact white light optical profiling system (WLOI) using VSI scanning (vertical scanning interferometry) with 20× magnification and an intermediate lens (FOV) 1×, controlled by WycoVision®32 analytical software package.

The most reported parameters to describe the roughness of the membrane surface are: the roughness average (R_a), the root-mean-square roughness (R_q), the average maxima profile height (R_z) and the maxima profile height (R_t) (Korkut et al., 2008; Mummery, 1993).

The R_a is the mean value of the surface height relative the centre plane, which is determined by equating the volumes enclosed by the image of the surface above and below the plane (Eq. (5)).

$$R_a = \frac{1}{N}\sum_{i=1}^{N} |Z_i| \tag{5}$$

where Z is the distance from the measured point to the mean plane and N is the number of points in the sample area.

The R_q is the root-mean-square roughness calculated over the entire measured array following the Eq. (6).

$$R_q = \sqrt{\frac{1}{N}\sum_{i=1}^{N} |Z_i^2|} \tag{6}$$

The peak-to-valley roughness, R_z, describes the average of the greatest peak-to-valley separations on the sample (Eq. (7)).

$$R_z = \frac{1}{N}\left(\sum_{i=1}^{N} H_i - \sum_{i=1}^{N} L_i\right) \tag{7}$$

where H_i is defined to be the ith highest point on the surface and L_i is defined to be the ith lowest point on the surface.

The maxima profile height, R_t, is the peak-to-valley difference calculated over the entire measured array following the Eq. (8).

$$R_t = R_p + R_v \tag{8}$$

where R_p (maxima profile peak height) is the distance between the highest point on the surface and the mean height of the surface, whereas R_v (maxima profile valley depth) is the distance between the lowest point on the surface and the mean height of the surface.

2.6.4. Study of volume recovery of calcium alginate hydrogel beads after dehydration and rehydration process

Calcium alginate hydrogel beads formulated with 2.2% sodium alginate at different concentrations of $CaCl_2$ (0.05, 0.475 and 0.9 mol L^{-1}) was submitted to 15 h dehydration at room temperature, followed by 8 h of rehydration and after this, optical images were obtained with a digital camera (Nikon) using macro view and controlled by a Image tool 3.00 software.

2.6.5. Thermo gravimetric analysis (TGA) of vineyard pruning waste entrapped in calcium alginate hydrogel beads

Thermo gravimetric analyses (TGA) of the vineyard-alginate biocomposite at different concentrations of $CaCl_2$ (0.05, 0.475 and 0.9 mol L^{-1}) were carried out on a thermal analyser SETSYS Evolution (Setaram Instrumentation). Samples were stored in deionized aqueous solution, thus before analysis calcium alginate hydrogel beads, containing vineyard pruning waste, were dried during 48 h at 60 °C in order to remove the excess of water. Following dry samples (10 mg) were heated from 25 to 550 °C at 10 °C min^{-1} under air with a flow rate of 30 mL min^{-1}.

2.7. Statistical analysis

The data obtained from the Box–Behnken factorial design were analysed using the STAT BASIC statistical program (Version 5.1 Statistic for Windows; Stat Soft, Inc., USA).

Data regarding the morphological study were analysed by analysis of variance (ANOVA) and significant differences were assessed by the Duncan's multiple range test at $p < 0.05$ using the IBM SPSS Statistics 20.0.0 statistical software package. Data are presented as the mean ± standard deviation ($n = 4$).

3. Results and discussion

3.1. Formulation of the vineyard-alginate biocomposite to remove dye compounds from wastewater

The cellulosic fraction of vineyard pruning waste was used in this work to prepare a biocomposite that can be used to remove dye compounds from industrial wastewater. This cellulosic residue was composed by 34.1% cellulose, 18.9% hemicelluloses and 27.1% lignin and after hydrolysis it was observed that the cellulosic fraction of vineyard pruning waste increased to 38.8% and the lignin to 40.2%.

Different concentrations of cellulosic residue, sodium alginate and $CaCl_2$ were tested in order to prepare a stable biocomposite with optima adsorbent capacities to eliminate dyes. Thus, a Box–Behnken incomplete factorial design was applied. Table 1 shows the independent variables studied consisting of cellulosic residue; sodium alginate and calcium chloride concentration; as well as the dependent variables analysed in this studied based on the decrease in the percentage of dye compounds and the increase of lightness measured as CI reduction (y_1) and L^* (y_2) respectively.

In Table 2 are included the percentages of dye compounds eliminated from wastewater measure as y_1 and the increase in lightness measured as y_2. Moreover, Table 2 also includes the statistical coefficients obtained after the treatment of the data. Thus, using these coefficients a quadratic function can be obtained for y_1 and y_2 where the percentage of dyes removed from wastewater can be calculated, in the range tested, by replacing the coefficients included in Table 2, in Eq. (9). Hence depending of the coefficients replaced in Eq. (9), y_1 or y_2 can be calculated.

Table 2
Experimental results and regression coefficients, with their statistical significance, achieved for the dependent variables y_1 and y_2.

Run	Independent variables (coded)			Dependent variables	
	x_1	x_2	x_3	y_1	y_2
1	0	−1	−1	84.32	91.71
2	0	1	−1	65.68	82.42
3	0	−1	1	86.59	92.86
4	0	1	1	75.05	86.34
5	−1	−1	0	72.44	85.48
6	−1	1	0	63.50	80.72
7	1	−1	0	77.40	88.14
8	1	1	0	78.95	88.70
9	−1	0	−1	69.56	84.03
10	−1	0	1	71.67	85.04
11	1	0	−1	79.94	89.40
12	1	0	1	85.36	92.24
13	0	0	0	80.77	89.62
14	0	0	0	80.76	89.69
15	0	0	0	80.92	88.64

Regression coefficients	Statistical significance			
	y_1	p_{y1}	y_2	p_{y2}
b_0	80.82	0.00000[a]	89.32	0.00001[a]
b_1	5.56	0.00003[a]	2.90	0.00508[a]
b_{11}	−4.51	0.00011[a]	−2.11	0.02041[a]
b_2	−4.70	0.00005[a]	−2.50	0.00682[a]
b_{22}	−3.23	0.00021[a]	−1.45	0.04160[a]
b_3	2.40	0.00018[a]	1.12	0.03295[a]
b_{33}	0.33	0.02042[a]	0.47	0.26621
b_{12}	2.62	0.00030[a]	1.33	0.04542[a]
b_{13}	0.83	0.00299[a]	0.46	0.25942
b_{23}	1.77	0.00066[a]	0.69	0.14229

It was observed a good correlation between the experimental results and the theoretical data predicted by the quadratic function with regression coefficient values, r^2, of 0.90 for y_1 and y_2.

[a] Significant coefficients ($p < 0.05$).

$$y = \beta_0 + \beta_1 x_1 + \beta_2 x_2 + \beta_3 x_3 + \beta_{12} x_1 x_1 + \beta_{13} x_1 x_3 + \beta_{23} x_2 x_3 + \beta_{11} x_1^2 + \beta_{22} x_2^2 + \beta_{33} x_3^2 \quad (9)$$

where y is the dependent variable (y_1 or y_2), β denotes the regression coefficients (calculated from experimental data by multiple regressions using the least-squares method) and x denotes the independent variables corresponding with x_1 (percentage of cellulosic residue), x_2 (percentage of sodium alginate) and x_3 (concentration of calcium chloride).

Fig. 1 shows the variation in the CI reduction (y_1) (Fig. 1a–c) and the L^* (y_2) (Fig. 1d–f), after treatment of wastewater using the vineyard-alginate biocomposite, with the most significant variables: concentration of cellulosic residue (x_1) and concentration of sodium alginate (x_2). The dye compounds in raw wastewater gave a CI of 2.04 and a L^* of 56.44. It was observed that concentrations of cellulosic residue higher than 1.25%, improved the adsorption capacity of the biocomposite to remove dye compounds from wastewater (deduced by the high L^* values obtained), whereas the highest concentrations of sodium alginate, in the range tested, gave lower L^* values. Thus, based on L^* values (y_2), vineyard-alginate biocomposite, with optimum adsorption capacity, can be formulated using 1.25% of cellulosic residue, 2.2% of sodium alginate and 0.475 mol L^{-1} of $CaCl_2$. Fig. 1d shows the variation of L^* using biocomposite formulated with the lowest concentration of $CaCl_2$ (0.05 mol L^{-1}); whereas Fig. 1e and f shows the same dependent variable when the $CaCl_2$ concentration was fixed at 0.475 mol L^{-1} and 0.9 mol L^{-1} respectively. The same conclusions were achieved when the reduction in the CI (y_1) was evaluated (Fig. 1a–c). Maxima reductions of CI (79.9–83.9%) were reached when the wastewater was treated with biocomposite formulated using intermediate to high doses of cellulosic residue and medium to low concentrations of sodium alginate.

Moreover, two extreme concentrations of $CaCl_2$ (0.05 and 0.9 mol L^{-1}) at the optima concentrations of cellulosic residue (1.25%) and sodium alginate (2.2%) were also studied in order to evaluate the regeneration capacity of the biocomposite. The $CaCl_2$ is the cross-linking solution that allows creating the calcium alginate hydrogel beads. The $CaCl_2$ concentration was the less significant variable on the CI reduction and L^* of wastewater; however, it can be an important parameter for controlling the hardness and the stability of the vineyard-alginate biocomposite. Table 3 shows the percentage of dyes removed after 3 cycles of adsorption–desorption using vineyard-alginate biocomposite formulated with different concentrations of $CaCl_2$ (0.05; 0.475 and 0.9 mol L^{-1}), 1.25% of cellulosic residue and 2.2% of sodium alginate. It was observed that vineyard-alginate biocomposite kept the adsorption capacity to remove dye compounds from winery

Table 3
CI reduction (y_1) and lightness (y_2) obtained after several cycles of adsorption–desorption using different optima formulations of the vineyard-alginate biocomposite.

	Color parameters	Formulation vineyard-alginate biocomposite*		
		Formulation 1	Formulation 2	Formulation 3
1st Adsorption	CI (%)	63.28	74.56	73.20
	L^* (Cielab units)	82.73	87.78	87.17
2nd Adsorption	CI (%)	62.19	63.68	60.11
	L^* (Cielab units)	81.99	82.62	80.98
3rd Adsorption	CI (%)	60.54	62.29	59.04
	L^* (Cielab units)	81.33	81.92	80.54

* Formulation 1: 1.25% cellulosic residue + 2.2% sodium alginate + 0.05 mol L^{-1} $CaCl_2$; Formulation 2: 1.25% cellulosic residue + 2.2% sodium alginate + 0.475 mol L^{-1} $CaCl_2$; Formulation 3: 1.25% cellulosic residue + 2.2% sodium alginate + 0.9 mol L^{-1} $CaCl_2$.

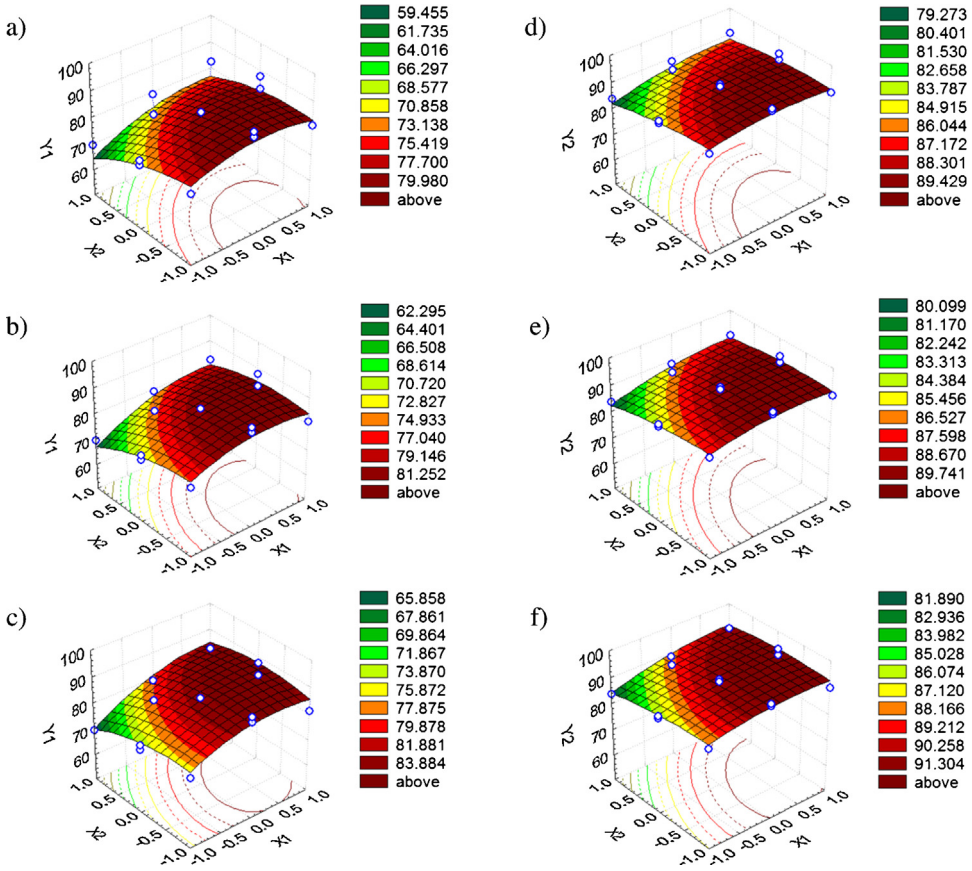

Fig. 1. Surface response variation of CI reduction (y_1) and L^* (y_2) in wastewater after treatment with the vineyard-alginate biocomposite formulated with different concentrations of cellulosic residue and sodium alginate concentration at a fixed concentration of $CaCl_2$ (a and d) 0.05 mol L^{-1}; (b and e) 0.475 mol L^{-1}; (c and f) 0.9 mol L^{-1}.

wastewater and no significant differences were found between samples after 3 cycles of adsorption–desorption.

In addition, Fig. 2 shows SEM images of the vineyard-alginate biocomposite, formulated at the optimum condition (1.25% of cellulosic residue, 2.2% of sodium alginate and 0.475 mol L^{-1} of $CaCl_2$) before and after the adsorption process. It was observed that the interstitial spaces of calcium alginate hydrogel beads, containing vineyard pruning waste, were filled up after the application of the biocomposite to the wastewater.

3.2. Morphology and surface properties of vineyard-alginate biocomposite

Area, perimeter, the major and the minor axis as well as the elongation, roundness and compactness of vineyard-alginate biocomposite were studied after various cycles of adsorption–desorption. Measurements of these parameters are included in Table 4. The biocomposite included in this table was formulated at the optima conditions predicted by the model following the Box–Behnken factorial design consisting of 1.25% of cellulosic, 2.2% of sodium alginate and three different concentrations of $CaCl_2$ 0.05; 0.475 and 0.9 mol L^{-1}. Moreover, calcium alginate hydrogel beads formulated only with 2.2% of sodium alginate and 0.05, 0.475 or 0.9 mol L^{-1} of $CaCl_2$, without cellulosic residue, were included in the surface properties study as controls.

The primary measuring information of image analysis methods is the contour of a particle. This makes up a difference to other techniques, for example, to laser diffraction or ultrasonic extinction, because the images contain information about the shape of

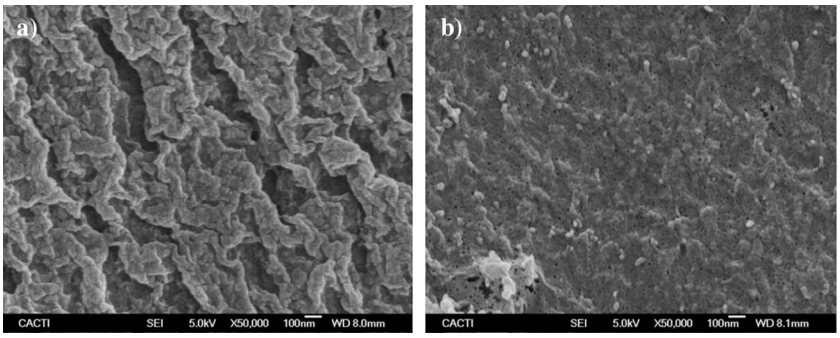

Fig. 2. SEM images of the vineyard-alginate biocomposite (a) before and (b) after the adsorption of dye compounds.

Table 4
Morphological properties of the calcium alginate hydrogel beads, containing vineyard pruning waste, under different formulations.

	Area (mm^2)	Perimeter (mm)	Major axis length (mm)	Minor axis length (mm)	Elongation (μm)	Roundness (μm)	Compactness (μm)
Formulation 1: 1.25% cellulosic residue + 2.2% sodium alginate + 0.05 mol L^{-1} $CaCl_2$							
Calcium alginate hydrogel beads	7.88 ± 1.42$^{c\ A}$	13.05 ± 2.54$^{b\ A}$	3.30 ± 0.40$^{c\ A}$	3.12 ± 0.29$^{b\ A}$	1.06 ± 0.03$^{b\ A}$	0.61 ± 0.16$^{b\ A}$	0.96 ± 0.03$^{a\ A}$
Vineyard-alginate biocomposite	19.32 ± 2.01$^{a,b\ A}$	17.70 ± 1.42$^{a\ A}$	5.13 ± 0.29$^{a,b\ A}$	4.89 ± 0.23$^{a\ A}$	1.05 ± 0.04$^{b\ B}$	0.78 ± 0.06$^{a\ A}$	0.97 ± 0.01$^{a\ A}$
1st Adsorption	17.02 ± 0.56$^{b\ A}$	16.70 ± 0.82$^{a\ A}$	4.96 ± 0.24$^{b\ A}$	4.61 ± 0.10$^{a\ A}$	1.08 ± 0.06$^{a,b\ A}$	0.77 ± 0.05$^{a\ A}$	0.94 ± 0.03$^{a,b\ A}$
2nd Adsorption	19.99 ± 4.63$^{a,b\ A}$	17.59 ± 2.10$^{a\ A}$	5.24 ± 0.82$^{a,b\ A}$	4.96 ± 0.52$^{a\ A}$	1.05 ± 0.06$^{b\ A}$	0.81 ± 0.01$^{a\ A}$	0.96 ± 0.04$^{a\ A}$
3rd Adsorption	21.68 ± 0.96$^{a\ A}$	18.90 ± 1.09$^{a\ A}$	5.90 ± 0.57$^{a\ A}$	5.02 ± 0.05$^{a\ A}$	1.18 ± 0.12$^{a\ A}$	0.77 ± 0.05$^{a\ A}$	0.90 ± 0.07$^{b\ A}$
Formulation 2: 1.25% cellulosic residue + 2.2% sodium alginate + 0.475 mol L^{-1} $CaCl_2$							
Calcium alginate hydrogel beads	8.18 ± 1.59$^{c\ A}$	12.12 ± 0.88$^{c\ A}$	3.39 ± 0.26$^{c\ A}$	3.19 ± 0.30$^{c\ A}$	1.07 ± 0.03$^{a\ A}$	0.69 ± 0.05$^{b\ A}$	0.95 ± 0.03$^{a\ A}$
Vineyard-alginate biocomposite	15.05 ± 1.19$^{a\ B}$	15.71 ± 0.64$^{a\ B}$	4.71 ± 0.19$^{a\ A,B}$	4.24 ± 0.26$^{a\ B}$	1.11 ± 0.05$^{a\ A,B}$	0.77 ± 0.03$^{a\ A}$	0.93 ± 0.03$^{a\ A,B}$
1st Adsorption	12.56 ± 1.40$^{a,b\ B}$	14.12 ± 1.07$^{b\ B}$	4.31 ± 0.47$^{a,b\ A}$	3.92 ± 0.18$^{a,b\ B}$	1.10 ± 0.10$^{a\ A}$	0.79 ± 0.04$^{a\ A}$	0.93 ± 0.05$^{a\ A}$
2nd Adsorption	10.84 ± 1.24$^{b\ B}$	13.12 ± 0.86$^{b,c\ B}$	4.00 ± 0.25$^{b\ B}$	3.65 ± 0.23$^{b,c\ B}$	1.10 ± 0.05$^{a\ A}$	0.79 ± 0.03$^{a\ A}$	0.93 ± 0.03$^{a\ A}$
3rd Adsorption	10.36 ± 2.51$^{b,c\ B}$	12.73 ± 1.42$^{b,c\ B}$	3.88 ± 0.44$^{b,c\ B}$	3.55 ± 0.42$^{b,c\ B}$	1.10 ± 0.08$^{a\ A}$	0.79 ± 0.01$^{a\ A}$	0.93 ± 0.04$^{a\ A}$
Formulation 3: 1.25% cellulosic residue + 2.2% sodium alginate + 0.9 mol L^{-1} $CaCl_2$							
Calcium alginate hydrogel beads	8.66 ± 1.10$^{b\ A}$	12.54 ± 2.08$^{a,b\ A}$	3.69 ± 0.54$^{a\ A}$	3.15 ± 0.20$^{c\ A}$	1.17 ± 0.14$^{a\ A}$	0.72 ± 0.16$^{a\ A}$	0.91 ± 0.09$^{a\ A}$
Vineyard-alginate biocomposite	12.94 ± 1.05$^{a\ B}$	14.70 ± 0.91$^{a\ B}$	4.46 ± 0.30$^{a\ B}$	3.94 ± 0.16$^{a\ B}$	1.13 ± 0.04$^{a\ A}$	0.75 ± 0.04$^{a\ A}$	0.91 ± 0.04$^{a\ B}$
1st Adsorption	11.47 ± 2.83$^{a,b\ B}$	13.48 ± 1.77$^{a,b\ B}$	4.15 ± 0.67$^{a\ A}$	3.76 ± 0.33$^{a,b\ B}$	1.10 ± 0.08$^{a\ A}$	0.79 ± 0.03$^{a\ A}$	0.92 ± 0.04$^{a\ A}$
2nd Adsorption	9.89 ± 1.68$^{b\ B}$	12.87 ± 1.32$^{a,b\ B}$	3.91 ± 0.30$^{a\ B}$	3.40 ± 0.40$^{b,c\ B}$	1.16 ± 0.10$^{a\ A}$	0.75 ± 0.06$^{a\ A}$	0.90 ± 0.04$^{a\ A}$
3rd Adsorption	9.23 ± 1.94$^{b\ B}$	12.10 ± 1.10$^{b\ B}$	3.72 ± 0.40$^{a\ B}$	3.31 ± 0.33$^{b,c\ B}$	1.12 ± 0.06$^{a\ A}$	0.78 ± 0.03$^{a\ A}$	0.92 ± 0.03$^{a\ A}$

Different lower case letters means significant differences, at $p < 0.05$, between samples for a particular formulation and for a specific parameter; whereas different capital letters means significant differences between formulations at the same adsorption cycle.

the particles (though two-dimensional only) in addition to the particle size.

When the elongation of an object is about 1 this is roughly circular or square. As the ratio increases from 1, the object becomes more elongated. In the three different formulations the vineyard-alginate biocomposite gave elongation values between 1.05 and 1.18.

Moreover, roundnesses obtained for the biocomposites studied in this work, gave values between 0.61 and 0.81. If the ratio is equal to 1, the object is a perfect circle, as the ratio decreases from 1 the object departs from a circular form.

It was observed that the biocomposite formulated with the cellulosic residue gave higher roundness values (0.75–0.81) than the control without the bioadsorbent (0.61–0.72), thus the cellulosic residue had a positive effect on the sharpness of the biocomposite corners.

On the other hand, when the compactness is equal to 1 the object is roughly circular, whereas as the ratio decreases from 1 the biocomposite becomes less circular. In this case compactness values of vineyard-alginate biocomposite were between 0.90 and 0.97. In general, it was observed that lower concentrations of $CaCl_2$ increased the compactness of the biocomposite.

Furthermore, the vineyard-alginate biocomposite formulated with lower amount of $CaCl_2$, 0.05 mol L^{-1}, increased the area of the biocomposite about 12.2% after 3 regeneration cycles, whereas when the biocomposite was formulated using $CaCl_2$ 0.475 mol L^{-1} and 0.9 mol L^{-1} the area of the biocomposite was reduced about 31.2% and 28.7% respectively. Thus, it can be deduced that $CaCl_2$ decreased the biocomposite flexibility providing higher hardness. These data are in concordance with the values achieved for the elongation, indicating that at higher concentrations of $CaCl_2$ less circle and more elongated biocomposites are obtained.

Moreover, Fig. 3 shows a macro view of the calcium alginate hydrogel beads, containing vineyard pruning waste, formulated with different concentrations of $CaCl_2$, at the beginning and after 3 adsorption–desorption cycles, in comparison with a control in absence of the cellulosic residue.

3.3. Surface roughness of calcium alginate hydrogel beads

The surface roughness can be an important parameter for evaluating the performance of a biocomposite, as it may influence the transport and adsorption process as well as other material characteristics such as the pore size distribution. For this reason the perfilometry study was carry out using calcium alginate hydrogel beads formulated under different concentrations of $CaCl_2$.

Roughness view depends on biocomposite height, diameter, shape, compliance, and density, thus the relationship between roughness perception and the physical properties of a surface is complex and non-linear. Roughness values can be calculated on a profile (line) or on a surface (area), being more usual the profile roughness parameters: R_a, R_q, R_z and R_t.

Fig. 4 shows representative two-dimensional (2D) and three-dimensional (3D) images of calcium alginate hydrogel beads formulated with different concentrations of $CaCl_2$. It can be observed that those calcium alginate hydrogel beads formulated with the lower concentration of $CaCl_2$ gave a surface free of irregularities, whereas in those beads formulated with 0.475 and 0.9 mol L^{-1} of $CaCl_2$ appeared vesicles in the surface.

Furthermore, in Table 5 are included the roughness parameters (R_a, R_q, R_z and R_t) of these 2D and 3D images. It can be observed that R_a and R_q values increased with the $CaCl_2$ concentration. Besides, using intermediate concentrations of $CaCl_2$ (0.475 mol L^{-1}), the calcium alginate hydrogel beads gave higher R_z and R_t values.

Table 5
Roughness parameters of calcium alginate hydrogel beads formulated with different concentrations of $CaCl_2$.

Roughness parameters (μm)	Calcium alginate hydrogel beads[a]		
	Formulation 1	Formulation 2	Formulation 3
R_a	0.12	1.01	1.03
R_q	0.18	1.29	1.36
R_z	3.56	25.14	14.16
R_t	5.48	33.77	26.13

[a] Formulation 1: 2.2% sodium alginate + 0.05 mol L^{-1} $CaCl_2$; Formulation 2: 2.2% sodium alginate + 0.475 mol L^{-1} $CaCl_2$; Formulation 3: 2.2% sodium alginate + 0.9 mol L^{-1} $CaCl_2$.

3.4. Volume recovery of calcium alginate hydrogel beads after dehydration and rehydration

Volume recovery is other important parameter in order to study the stability of the composite. Fig. 5a shows calcium alginate hydrogel beads without any dehydration process, whereas Fig. 5b shows the hydrogel beads after 15 h of dehydration at room temperature. It was observed a linear relationship between the decrease of the hydrogel bead volume and the concentration of $CaCl_2$ after dehydration. Thus, calcium alginate hydrogel beads formulated with 0.05 mol L^{-1} $CaCl_2$ lost 60% of the volume, whereas hydrogel beads formulated with 0.475 mol L^{-1} and 0.9 mol L^{-1} $CaCl_2$ lost 54.1% and 47.4% respectively. Furthermore, Fig. 5c shows the volume achieved by the calcium alginate hydrogel beads after 15 h of dehydration followed by 8 h of rehydration. The hydrogel beads formulated with 0.05 mol L^{-1} $CaCl_2$, shown in Fig. 5c, recovered 25% of volume in comparison with the dehydrated calcium alginate hydrogel beads, shown in Fig. 5b, whereas hydrogel beads formulated with 0.475 mol L^{-1} and 0.9 mol L^{-1} $CaCl_2$ recovered 17.6% and 10% of the volume respectively. Results achieved in this study corroborate that calcium alginate hydrogel beads formulated with the lowest concentration of $CaCl_2$ are more flexible allowing a better volume recovery.

3.5. TGA analysis

TGA curves of the vineyard pruning waste entrapped in calcium alginate hydrogel beads are shown in Fig. 6. It was observed that biocomposites did not have a noticeable weight loss until the temperature reached 200 °C, may be due to the pretreatment of vineyard-alginate biocomposites at 60 °C. Afterwards, from 200 °C to 525 °C, biocomposites were decomposed sharply, observing that

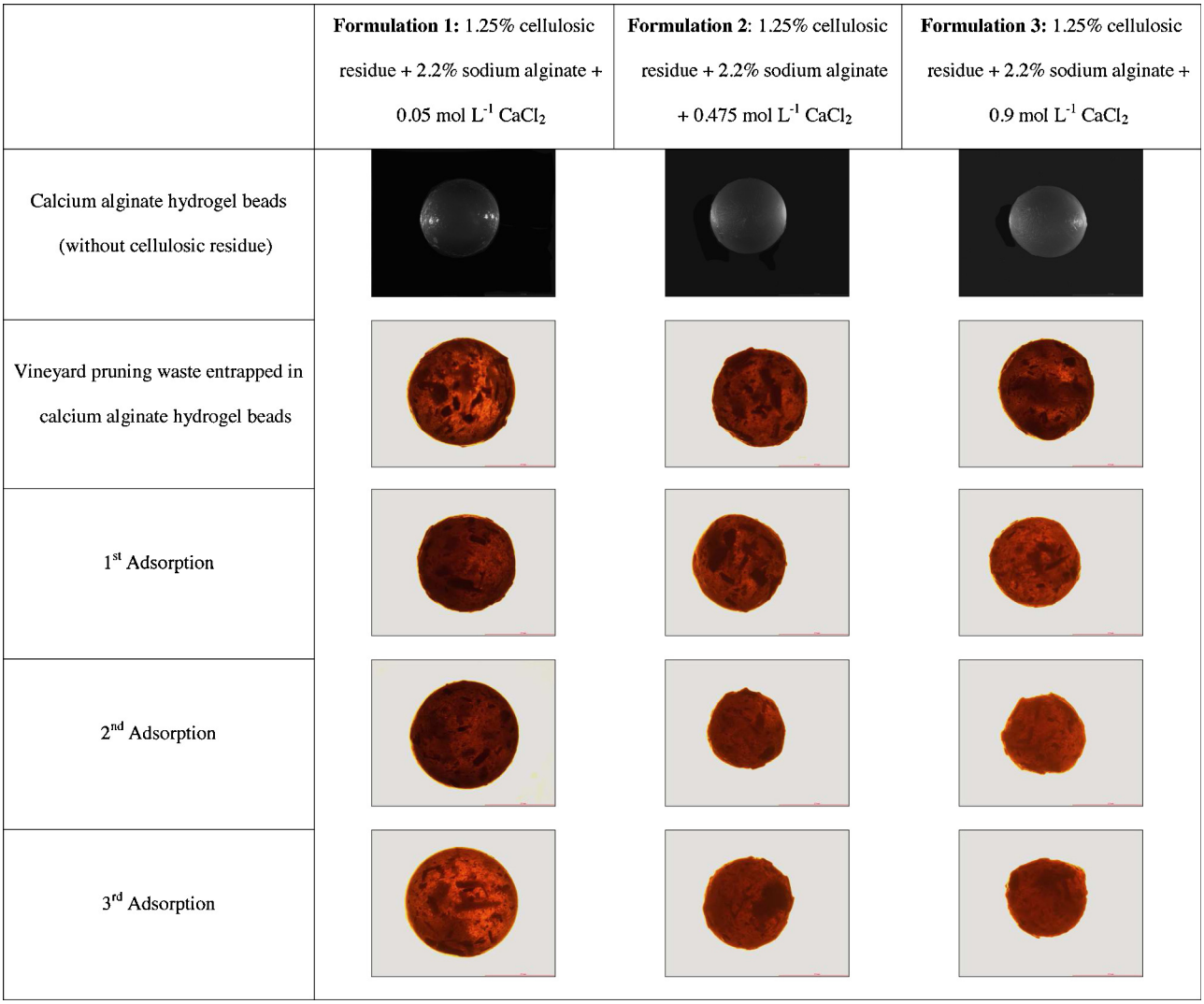

Fig. 3. Macro view of the calcium alginate hydrogel beads, containing vineyard pruning waste, formulated using different concentrations of $CaCl_2$, at the beginning and after 3 regeneration cycles, in comparison with a control in absence of the cellulosic residue.

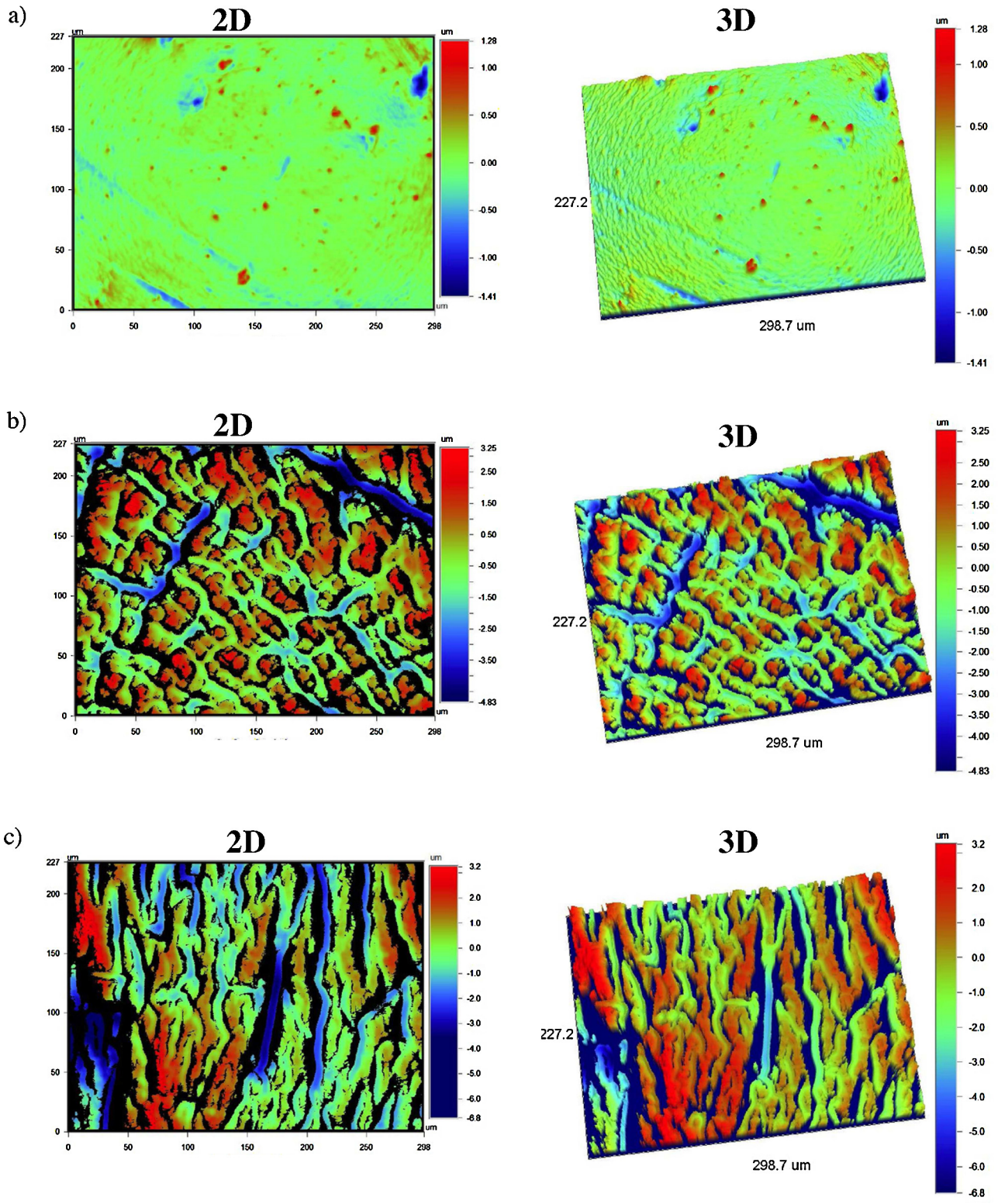

Fig. 4. Surface roughness at two-dimensional (2D) and three-dimensional (3D) images of the calcium alginate hydrogel beads formulated with different concentrations of $CaCl_2$: (a) 0.05 mol L^{-1}, (b) 0.475 mol L^{-1} and (c) 0.9 mol L^{-1}.

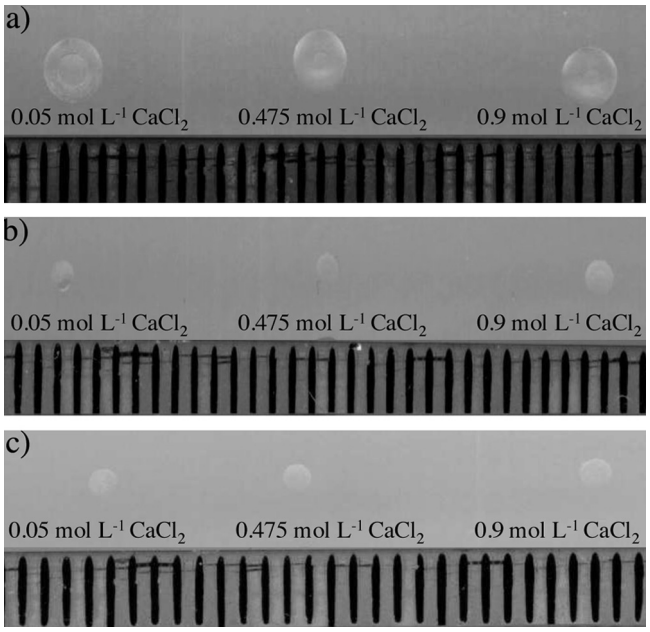

Fig. 5. Images of calcium alginate hydrogel beads formulated with different concentrations of $CaCl_2$: (a) initial state of the hydrogel beads; (b) after 15 h of dehydration at room temperature and (c) after 8 h of rehydration.

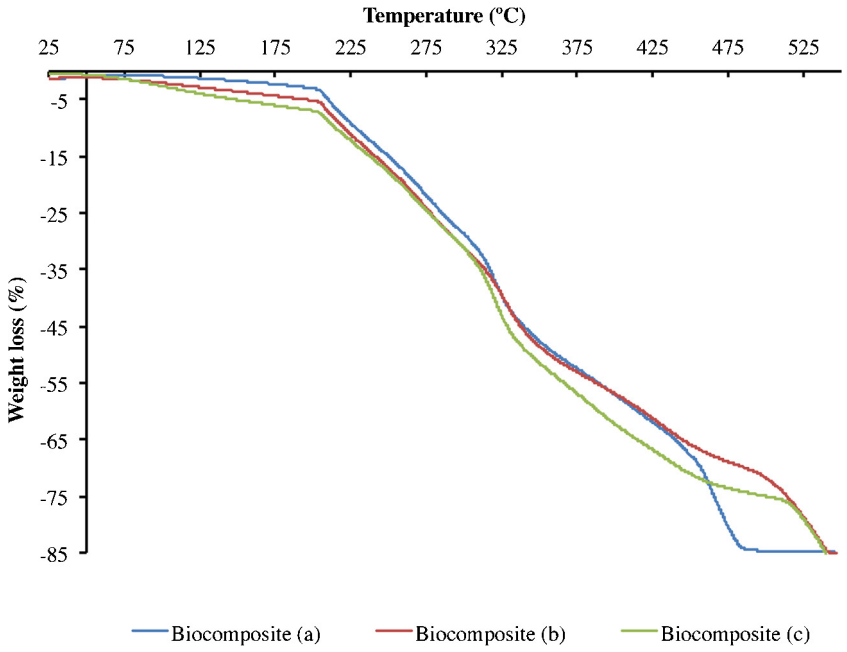

Fig. 6. TGA curves of vineyard-alginate biocomposites at different $CaCl_2$ concentrations: (a) 0.05 mol L^{-1}, (b) 0.475 mol L^{-1} and (c) 0.9 mol L^{-1}.

most of the organic functional moieties included in the polymer matrix were thermally unstable over 200 °C. In addition, TGA study showed that the thermal stability of vineyard-alginate biocomposite got increased with medium-high concentration of $CaCl_2$ in the polymer matrix.

4. Conclusions

Results obtained in this study suggest that the vineyard pruning waste entrapped in calcium alginate hydrogel beads formulated in this work may provide a promising eco-friendly and cleaner alternative to replace the existing no renewable adsorbents. The removal efficiency of dyes from wastewater was affected by the concentration of the cellulosic residue and sodium alginate doses used in the formulation of the vineyard-alginate biocomposite. The $CaCl_2$ concentrations used during the formulation of the bioadsorbent provided the less significant effect in the elimination of dyes from wastewater. Moreover, it was observed that higher doses of $CaCl_2$ increased the roughness and gave less circle hydrogel beads although it did not affect the biocomposite adsorption capacity. Finally, morphology and surfaces analysis of the calcium alginate hydrogel beads, containing vineyard pruning waste, formulated at the optimum condition (1.25% of cellulosic residue, 2.2% of sodium alginate, 0.475 mol L^{-1} $CaCl_2$), revealed that the vineyard-alginate biocomposite was very stable, keeping elongation, roundness and compactness values constant after various regeneration cycles.

Acknowledgements

Authors wish to thank the Spanish Ministry of Economy and Competitiveness (project CTM2012-31873) and Vecino X. gratefully acknowledges the University of Vigo for her predoctoral contract.

References

Avérous, L., & Le Digabel, F. (2006). Properties of biocomposites based on lignocellulosic fillers. *Carbohydrate Polymers*, *66*, 480–493.

Berns, R. (2000). *Billmeyer and Saltzman's principles of color technology* (3rd ed.). New York: John Wiley & Sons.

Box, G. E. P., & Behnken, D. W. (1960). Simplex-sum designs – A class of 2nd order rotatable designs derivable of those of 1st order. *Annals of Mathematical Statistics*, *31*, 838–864.

Bustos, G., Moldes, A. B., Cruz, J. M., & Domínguez, J. M. (2004). Production of fermentable media from vine-trimming wastes and bioconversion into lactic acid by *Lactobacillus pentosus*. *Journal of the Science of Food and Agriculture*, *84*, 2105–2112.

Cruz, J. M., Moldes, A. B., Bustos, G., Torrado, A., & Domínguez, J. M. (2007). Integral utilisation of barley husk for the production of food additives. *Journal of the Science of Food and Agriculture*, *87*, 1000–1008.

Devesa-Rey, R., Bustos, G., Cruz, J. M., & Moldes, A. B. (2011). Optimisation of entrapped activated carbon conditions to remove coloured compounds from winery wastewaters. *Bioresource Technology*, *102*, 6437–6442.

Gonte, R. R., Shelar, G., & Balasubramanian, K. (2013). Polymer-agro-waste composites for removal of Congo red dye from wastewater: Adsorption isotherms and kinetics. *Desalination and Water Treatment*, 1–15.

Janaki, V., Vijayaraghavan, K., Ramasamy, A. K., Lee, K. J., Oh, B. T., & Kamala-Kannan, S. (2012). Competitive adsorption of reactive orange 16 and reactive brilliant blue R on polyaniline/bacterial extracellular polysaccharides composite-A novel eco-friendly polymer. *Journal of Hazardous Materials*, *241–242*, 110–117.

Kalia, S., Dufresne, A., Mathew Cherian, B., Kaith, B. S., Avérous, L., Njuguna, J., et al. (2011). Cellulose-based bio- and nanocomposites: A review. *International Journal of Polymer Science*, 1–35.

Korkut, D. S., Korkut, S., Bekar, I., Budakçi, M., Dilik, T., & Çakicier, N. (2008). The effects of heat treatment on the physical properties and surface roughness of Turkish Hazel (*Corylus colurna* L.) wood. *International Journal of Molecular Sciences*, *9*, 1772–1783.

Moldes, A. B., Torrado, A., Converti, A., & Domínguez, J. M. (2006). Complete bioconversion of hemicellulosic sugars from agricultural residues into lactic acid by *Lactobacillus pentosus*. *Applied Biochemistry and Biotechnology*, *135*, 219–227.

Moldes, A. B., Torrado, A. M., Barral, M. T., & Domínguez, J. M. (2007). Evaluation of biosurfactant production from various agricultural residues by *Lactobacillus pentosus*. *Journal of Agricultural and Food Chemistry*, *55*, 4481–4486.

Mummery, L. (1993). Surface texture analysis. In *The handbook*. Muhlhausen, Germany: Hommelwerke.

Perez-Ameneiro, M., Vecino, X., Barbosa-Pereira, L., Cruz, J. M., & Moldes, A. B. (2014). Removal of pigments from aqueous solution by a calcium alginate-grape marc biopolymer: A kinetic study. *Carbohydrate Polymers*, *101*, 954–960.

Rivas, B., Torrado, A., Rivas, S., Moldes, A. B., & Domínguez, J. M. (2007). Simultaneous lactic acid and xylitol production from vine trimming wastes. *Journal of the Science of Food and Agriculture*, *87*, 1603–1612.

Rivera, O. M. P., Moldes, A. B., Torrado, A. M., & Domínguez, J. M. (2007). Lactic acid and biosurfactants production from hydrolyzed distilled grape marc. *Process Biochemistry*, *42*, 1010–1020.

Thakur, M. K., Gupta, R. K., & Thakur, V. K. (2014). Surface modification of cellulose using silane coupling agent. *Carbohydrate Polymers*, *111*, 849–855.

Thakur, V. K., Thakur, M. K., & Gupta, R. K. (2013a). Development of functionalized cellulosic biopolymers by graft copolymerization. *International Journal of Biological Macromolecules*, *62*, 44–51.

Thakur, V. K., Thakur, M. K., & Gupta, R. K. (2013b). Graft copolymers from cellulose: Synthesis, characterization and evaluation. *Carbohydrate Polymers*, *97*, 18–25.

Thakur, V. K., Thakur, M. K., & Gupta, R. K. (2013c). Rapid synthesis of graft copolymers from natural cellulose fibers. *Carbohydrate Polymers*, *98*, 820–828.

Thakur, V. K., Thakur, M. K., & Gupta, R. K. (2013d). Synthesis of lignocellulosic polymer with improved chemical resistance through free radical polymerization. *International Journal of Biological Macromolecules*, *61*, 121–126.

Thakur, V. K., Thakur, M. K., & Gupta, R. K. (2014). Graft copolymers of natural fibers for green composites. *Carbohydrate Polymers*, *104*, 87–93.

Tran, C. D., Duri, S., Delneri, A., & Franko, M. (2013). Chitosan-cellulose composite materials: Preparation, characterization and application for removal of microcystin. *Journal of Hazardous Materials*, *252-253*, 355–366.

Vecino, X., Devesa-Rey, R., Cruz, J. M., & Moldes, A. B. (2013). Entrapped peat in alginate beads as green adsorbent for the elimination of dye compounds from vinasses. *Water Air and Soil Pollution*, *224*, 1–9.

Vecino, X., Devesa-Rey, R., Moldes, A. B., & Cruz, J. M. (2012). Optimization of batch operating conditions for the decolourization of vinasses using surface response methodology. *Microchemical Journal*, *102*, 83–90.

Völz, H. G. (2001). *Industrial color testing*. Weinheim: Wiley-VCH.